

Disposable Endoscope Tip Actuation Design and Robotic Platform

Yi Chen, Shigehiko Tanaka, and Ian W. Hunter

Abstract—A disposable endoscopic platform with actuation motors inside the body of the endoscope is presented. This platform can enable new medical devices for diagnosis and for minimally invasive surgeries. This paper addresses mechanical and safety issues with existing endoscope technologies by incorporating disposability, safety modules, and lower cable forces. In order to produce path-independent cable forces, motors are incorporated in the body of the endoscope near the bending tip. Results for tip forces are shown accompanied by an analytical model describing the scaling laws for this type of robotic architecture. The system under development will provide a platform for research into haptic control and perceptual feedback.

I. INTRODUCTION

ENDOSCOPIC procedures have become common medical practice for visual diagnosis, biopsy and polyp/tumor removal. Recent medical innovations in minimally invasive surgery (MIS), natural orifice transluminal endoscopic surgery (NOTES), and other next generation medical devices suggest the need for new platform technologies. In MIS and NOTES, the small workspaces and inhibited manual dexterity necessitate the use of robotic systems for more accurate and tremor free procedures. Research in this area includes robotic assisted surgery [1, 2], haptic control [3], and tools for minimally invasive surgery [4, 5]. In general, research devices are added directly to existing endoscopic systems [4], which limit the control strategies and the range of tools that can be implemented. Recent commercial devices in this area include the da Vinci Surgical System laparoscope by Intuitive Surgical Inc. which allows for robotic-assisted operations [6]. The platforms currently in use in systems like the da Vinci are large, expensive, and not suited for conventional diagnostics. The platform proposed in this paper will hopefully bring innovations from intricate robotic-assisted surgeries to routine endoscopic diagnostics.

The proposed endoscopic system has two main goals: 1) to alleviate some of the fundamental issues plaguing existing endoscopic systems and 2) to create a robotic platform that will enable the next generation of medical procedures. Any new design should first attempt to address the issues of previous designs. Based on medical device safety reports collected by the FDA from 1985 to 2009 on colonoscopies [7, 8], the most commonly reported mechanism failures are

those due to image loss (contamination and CCD failure, ~67%), cable malfunctions (broken and snagged control cables and pulleys, ~21%), and scope structural breakage during a procedure (due to overuse and improper handling, ~5%). The most common medical issues associated with endoscopes include bowel perforations (due to stiff scopes or pre-existing patient conditions, ~64%), glutaraldehyde and other chemical colitis (due to inadequately rinsed auxiliary passages, ~18%), and cross contaminations and infections (from improperly cleaned endoscopes, ~9%).

Based on these reports, several changes can be proposed. First, a disposable endoscope architecture will have the largest impact on reducing these complaints. This architecture can mitigate or eliminate problems associated with the chemical colitis, cross contamination, overuse and improperly performed repairs. Having more disposable parts will also reduce the burden on the hospital by reducing the size of the cleaning machines, the turn-around time for the use of scopes, and the need for a dedicated staff member to clean scopes. Due to the inherent cost of certain components of the endoscopic system, it is not economically feasible to dispose of all sections of an endoscope. Prior art, that attempts to address these issues, includes many disposable sheath endoscopes [9,10], disposable rigid endoscope optics [11] and entirely disposable systems. Secondly, different actuation architectures with actuation motors near the tip of the endoscope can be used to address the cable failure and bowel perforation problem by shortening cable length and decreasing cable forces. Robotic actuation systems can be used to provide accuracy [6], sensory feedback [3], and additional safety features. Endoscopes and catheters with a variety of drive strategies [12, 13, 14] exist but do not directly address the issues in existing endoscopes.

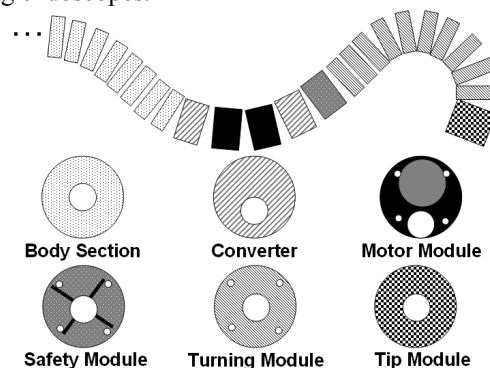


Fig. 1. Modular concept for endoscope design. Geometry for the tool channel, control strings, and motor location are shown. Auxiliary ports and features are not shown for clarity. Module lengths are not to scale.

Manuscript received April 1, 2010 for the IEEE EMB Conference.

Y. Chen, and I. W. Hunter are with the Department of Mechanical Engineering at Massachusetts Institute of Technology, Cambridge, MA 02139 USA (phone: 617-233-4292; e-mail: yichen@mit.edu).

S. Tanaka is a visiting scholar at Massachusetts Institute of Technology, Cambridge, MA 02139 USA.

This paper presents new methods that address disposability and robotic endoscope actuation with motors that fit inside the body of the endoscope near the actuated tip. Design rationalization, modeling concepts, and experimental data will be presented. With the use of this platform, new features such as touch feedback, real-time fluoroscopy and spectroscopy can also be realized.

II. DESIGN

A. Conceptual Design

The modular design shown in Figure 1 was selected to reduce manufacturing cost and permit simple adjustment in length. This design allows for the disposal of the most difficult-to-clean sections of the endoscope from the body section through the turning modules. It also allows for the non-disposable tip module to be sealed separately, thereby mitigating contamination. The body section incorporates variable stiffness, which is a feature that appears in existing endoscope designs [4]. Variable stiffness allows the endoscope to be stiffened when it enters the body so that it can be easily inserted and advanced. When the endoscope exits the body, the stiffness can be reduced so that it can be easily withdrawn from the body without causing damage and so that loops in the endoscope can be resolved. In addition, the variable stiffness can be dialed below the perforation threshold for patients with pre-existing tissue fragility.

The design of the turning section includes rubber spacers and acrylic modules with four nylon control strings. The turning angle and internal stiffness of this section can be modulated by the lengths and diameters of the turning modules and spacers. This type of un-jointed system was selected over a jointed system [15, 16] because jointed systems tend to be stiffer and more difficult to move, requiring higher forces. An un-jointed system is more flexible to accommodate patient breathing motion and to reduce the occurrence of bowel perforations.

The safety module is added to cut strings in the event that the motors malfunction while the tip is bent. The tip module includes the imaging system, CCD, and LED light sources. Additional instruments for biopsy and other procedures can be passed down the tool channel.

B. Actuation Mechanics

Cable drive systems often require high forces when actuated from the end of the endoscope. Pulling the cables becomes exponentially harder as the number of turns in the body increases due to capstan friction. The proposed system incorporates the motors near the tip of the endoscope creating significant benefits. Because the motors are closer to the tip, the forces necessary to turn the tip will be smaller and will be independent of the number of bends made in the body. This has additional benefits for haptic control and perceptual feedback systems. The forces created by the smaller motor at the tip of the endoscope also make it less likely to snap the cables. In addition, it becomes easier to design the system for limiting the maximum forces, making

it impossible to accidentally overdrive the motor and perforate healthy bowel walls. An additional benefit to this design is that the motor and turning modules can be repeated to allow for multiple controllable articulation points.

Several designs for the structure of the motor articulation were considered including the use of a linear Lorentz force voice coil, lead screw and nut [15], and stepper motor with internal flexible lead screw. In order to reduce cost, minimize motor module length and be able to hold a fixed position without using power, a design with a pre-existing 6 mm diameter geared rotary motor with direct cable transmission was chosen. The current gearmotor has a stall torque of 1.08 mNm at 3 V. The motor module is less than 30 mm in length and 11 mm in diameter. The design for the rotary to linear transmission for the motion of the cable is shown in Figure 2.

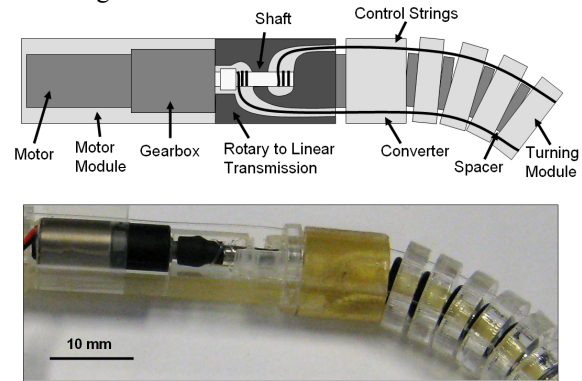


Fig. 2. Motor actuation system conceptual design and implementation without outer sheath. The transmission of the system changes the rotary motion of the geared motor into linear motion in the two opposing cables.

When one of the strings is pulled by the transmission, the other string is released thereby allowing the endoscope tip to bend. Since two strings in opposing action are wound about each shaft, the cable pulling rotation cannot be accidentally reversed. When the maximum bending angle is reached, the motor is designed to stall. Because of gear box resistance and geometric constraints, this design can hold a position without the use of power. Each of the cardinal directions can be bent up to 180° and two motors acting in tandem can access space 360° around the tip, which is in line with the capabilities of conventional endoscopes.

C. Software and Electronics

The drive electronics for this system uses H-bridges and an adjustable pulse width modulation (PWM) in order to obtain higher instantaneous torques and for speed control of the two degrees of motion. A Logitech® Attack™ 3 joystick and software written in NI LabVIEW 8.5 are used to control the position of tip of the endoscope.

III. MODELING

The force that the tip of the endoscope system can produce determines the maneuverability of the system. However, the tip force should not exceed the perforation force of healthy tissue (in the case of operator error).

Therefore, a model that can be used to guide the selection of the geared motor and articulated tip dimensions is necessary.

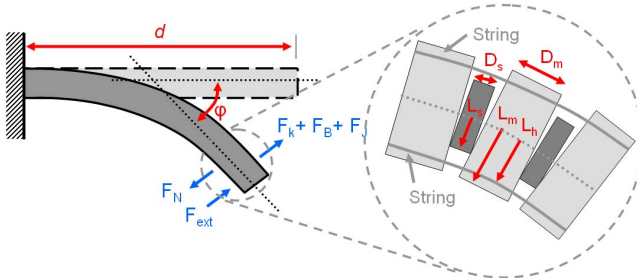


Fig. 3. Geometry of model for angle to tip force relationship.

The maximum bending angle is defined by the relative sizes of the beads and spacers. For n spacers with length D_s and radius L_s , and module radius of L_m , a first order estimate of the maximum bending angle can be obtained,

$$\varphi_{\max} = 2n \sin^{-1} \left(\frac{D_s}{2(L_m - L_s)} \right). \quad (1)$$

By balancing forces at the tip of the endoscope in the normal direction, it is possible to obtain Equation 2. The forces, in order, are the externally applied normal force (which is measured), the force associated with the spring constant, the force associated with damping, the force associated with inertia, and the internal normal force from cable tension. Results from other configurations with additional contact forces can be derived similarly.

$$F_{\text{ext}} + F_k + F_B + F_J - F_N = 0 \quad (2)$$

From experimental data, we find that the spring force is $F_k = K\varphi$, damping force is $F_B = B\dot{\varphi}$ and inertial force is $F_J = J\ddot{\varphi}$. Note that Equation 2 only exists for positive values of F_N and F_{ext} since the string pulling procedure produces forces in only one direction. The internal normal force from string tension is related to the tangential string tension and this relation can be derived with a torque balance for the tip module at the very end. The tip force can be approximated using the capstan friction equation where μ is the coefficient of friction, F_{in} is the force output of the motor, and F_{tip} is the force measured at the tip. An extra $\pi/2$ term occurs due to the capstan friction in the 90° turn inside the rotary to linear transmission. This is shown in Equation 3.

$$F_N = \frac{L_h - L_s}{D_m + D_s} F_{\text{tip}} = \frac{L_h - L_s}{D_m + D_s} F_{\text{in}} e^{-\mu(\varphi + \frac{\pi}{2})} \quad (3)$$

The input force can be measured or calculated from first principles using the input voltage V , gear ratio N , motor constants K_e and K_t , radius of the motor shaft r , resistance of the motor R , and angle of the motor shaft θ . Equation 4 shows this relation,

$$F_{\text{in}} = NK_t \frac{V - K_e \dot{\theta} / N}{Rr}. \quad (4)$$

The full dynamics can be obtained in Equation 5,

$$F_{\text{ext}} = \frac{L_h - L_s}{D_m + D_s} \left(NK_t \frac{V - K_e \dot{\theta} / N}{Rr} \right) e^{-\mu(\varphi + \frac{\pi}{2})} - K\varphi - B\dot{\varphi} - J\ddot{\varphi}. \quad (5)$$

A relationship between the motor angle and bending angle can be derived from geometry. The relationship shown in Equation 6 is valid up to φ_{\max} . The approximation on the right can be used for small φ/n ,

$$\theta = \frac{n(L_h - L_s)}{r} \sin(\varphi/n) \approx \frac{(L_h - L_s)}{r} \varphi. \quad (6)$$

For a static system, Equation 5 reduces to Equation 7 for an input torque of T_{in} ,

$$F_{\text{ext}} = \frac{L_h - L_s}{D_m + D_s} \frac{T_{\text{in}}}{r} e^{-\mu(\varphi + \frac{\pi}{2})} - K\varphi. \quad (7)$$

The spring constant K is a function of the elasticity of endoscope tip (including the tool channel material, wire and tubing), the moment of inertia, and the length of the endoscope tip d . Experimental data can be used to validate the theory and to produce designs with the desired force and speed characteristics.

IV. RESULTS

The forces exerted by the endoscope tip were tested by holding the motor module fixed and measuring the force against the tip at different bending angles. The results of the test along with the analytical model for the static tip force are plotted on Figure 4a.

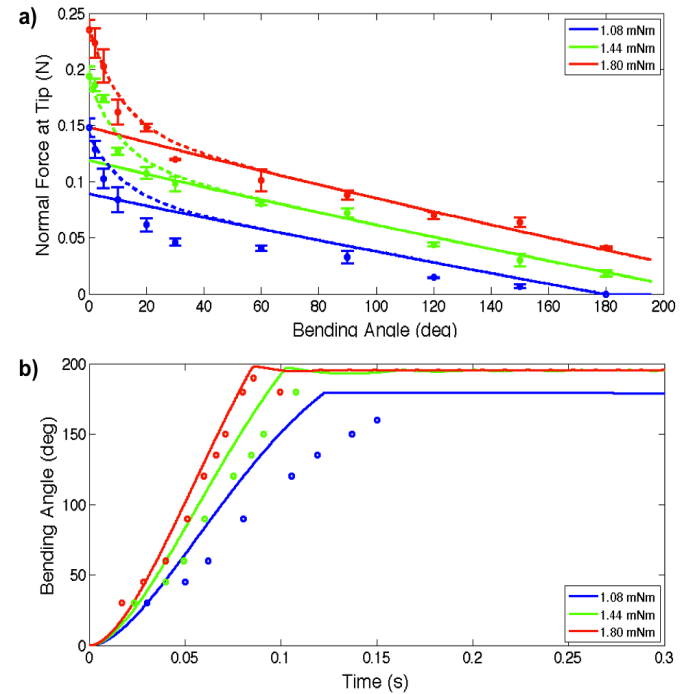


Fig. 4. a) Static normal forces at the tip as a function of the bending angle for different input torques. The dots with standard deviation bars represent experimental data, the solid lines represent model predictions, and the dotted lines represent model predictions with the low angle correction. b) Bending angle as a function of time for different input torques. The dots represent experimental data and the lines represent model fits. The dimensions were chosen based on iterative design with 6 mm motors: $n = 11$, $r = 1.1$ mm, $D_s = 0.7$ mm, $D_m = 2.9$ mm, $L_s = 3.3$ mm, $L_m = 5.5$ mm, and $L_h = 3.7$ mm.

The measured spring constant is 0.020 N/rad, the measured coefficient of static friction is 0.28 rad⁻¹, and the measured coefficient of sliding friction is 0.10 rad⁻¹. The experimental data with standard deviation bars matches well with the predicted output for larger angles, but a low angle correction of the form $(1+C_1\exp(-C_2\phi))$ is necessary for smaller angles. At low angles, the string tension has more leverage than predicted by the model because the play in the hole for the string allows the selection of different bending points. The correction factor, which represents the exponentially decreasing leverage from string tension, is multiplied with the tip force.

In addition to the static tip forces, the dynamics of the endoscope can also be plotted using the dynamic model with $F_{\text{ext}} = 0$, and this is shown in Figure 4b. This is validated with experimental data from high speed camera images at 600 fps (representative points plotted) taken of the system at different input torques associated with different input voltages. As the input torque increases, the endoscope tip approaches the maximum bending angle more quickly. If the motor voltage is too low, the endoscope is incapable of reaching the maximum angle. When the endoscope tip reaches the angle limit, the tip oscillates slightly by deforming in directions out of the plane of cable actuation. The fitted values for the dynamic model are $J = 9.0 \times 10^{-5} \text{ N/(s}^2\cdot\text{rad)}$ and $B = 1.5 \times 10^{-3} \text{ N/(s}\cdot\text{rad)}$.

In order to assess the design, the tip forces are compared to the critical contact pressures of human organs, which are on the order of 20 kPa [17]. This indicates that the resistive force of the organ is at minimum 0.64 N for a tip module of 11 mm in diameter and 2.9 mm in length. The current model produces forces well below this value and additional design based on this model can prevent forces from reaching critical contact pressures in possible failure modes. Conventional endoscope designs with longer cable actuation mechanisms are susceptible to additional forces from bends in the body of the endoscope. The motor torques for these systems are much higher and the operator is more likely to produce tip forces that could potentially puncture organs.

V. CONCLUSION

The concepts presented in this paper constitute an advance over previous work [16] and have the potential to solve many of the existing problems with endoscopes as well as provide a new platform for haptic control and next-generation endoscope tools. A novel motor drive system is presented along with a model for tip deflection and forces. The results match well with predicted performance and provide a good springboard for design optimization.

Future work in this area will include the design and implementation of a haptic control system along with the development of new endoscope tools. Finally, *in vivo* testing will be conducted. It is hoped that the mechanical architecture presented in this paper will inspire future development of endoscopic devices and tools.

ACKNOWLEDGMENT

The authors would like to thank Bryan Ruddy for his preliminary work and for his invaluable advice. We would also like to thank Al Couvillon, Dr. Cathy Hogan, Dr. Lynette Jones, and other members of the BioInstrumentation Lab for their assistance. This project was funded by a fellowship from the National Science Foundation.

REFERENCES

- [1] H. Mayer, I. N. A. Knoll, E. U. Braun, R. Bauernschmitt, and R. Lange, "Haptic feedback in a telepresence system for endoscopic heart surgery," *Presence*, vol. 16, No. 5, pp. 459-470, 2007.
- [2] S. J. Phee, S. C. Low, V. A. Huynh, A. P. Kencana, Z. L. Sun, and K. Yang, "Master and slave trasluminal Endoscopic robot (MASTER) for natural orifice trasluminal endoscopic surgery (NOTES)," *31st Annual International Conference of the IEEE Engineering in Medicine and Biology Society*, pp. 1192-1195, 2009.
- [3] M. Tavakoli, R. V. Patel, and M. Moallem, "Haptic interaction in robot-assisted endoscopic surgery, a sensorized end-effector," *International Journal of Medical Robotics and Computer Assisted Surgery*, vol. 1, No. 2, pp. 53-63, 2005.
- [4] B. Bardou, F. Nageotte, P. Zanne, and M. De Mathelin, "Design of a telemanipulated system for transluminal surgery," *31st Annual International Conference of the IEEE Engineering in Medicine and Biology Society*, pp. 5577-5582, 2009.
- [5] J. Rosen, B. Hannaford, M. MacFarlane, and M. Sinanan, "Force controlled and teleoperated endoscopic grasper for minimally invasive surgery – experimental performance evaluation," *IEEE Transactions on Biomedical Engineering*, vol. 46, No.10, pp. 1212-1221, 1999.
- [6] B. T. Bethea, A. M. Okamura, M. Kitagawa, T. P. Fitton, S. M. Cattaneo, V. L. Gott, W. A. Baumgartner, and D. D. Yuh, "Application of haptic feedback to robotic surgery," *Journal of Laparoendoscopic & Advanced Surgical Techniques*, vol. 14, No. 3, pp. 191-195, 2004.
- [7] Medical Device Reporting, U. S. Food and Drug Administration, [Online] Available: <http://www.accessdata.fda.gov/scripts/cdrh/cfdocs/cfMDR/Search.cfm>, [Accessed: October 23, 2009].
- [8] Manufacturer and User Facility Device Experience, U. S. Food and Drug Administration, [Online] Available: <http://www.accessdata.fda.gov/scripts/cdrh/cfdocs/cfMAUDE/search.CFM>, [Accessed: October 23, 2009].
- [9] R. I. Rothstein and B. Littenberg, "Disposable, sheathed, flexible sigmoidoscopy: A prospective, multicenter, randomized trial," *Gastrointestinal Endoscopy*, vol. 41, pp. 566-572.
- [10] E. A. Opie, E. J. Terry, F. E. Silverstein, "Endoscope for use with a disposable sheath," U. S. Patent 4,869,238, September 26, 1989.
- [11] B. G. Broome, "Disposable endoscope," U. S. Patent 5,341,240A, August 23, 1994.
- [12] Y. Chen, J. H. Chang, A. S. Greenlee, K. C. Cheung, A. H. Slocum, and R. Gupta, "Multi-turn, tension-stiffening catheter navigation," *Proceedings of 2010 IEEE International Conference on Robotics and Automation*, pp. 5570-5575, 2010.
- [13] M. P. Armacost, J. Adair, T. Munger, R. R. Viswanathan, F. M. Creighton, D. T. Curd, and R. Sehra, "Accurate and reproducible target navigation with Stereotaxis Niobe magnetic navigation system," *Journal of Cardiovascular Electrophysiology*, vol. 18, pp. 26-S31, 2007.
- [14] P. Kanagaratnam, M. Koa-Wing, D. T. Wallace, A. S. Goldenberg, N. S. Peters, and D. W. Davies, "Experience of robotic catheter ablation in humans using a novel remotely steerable catheter sheath," *Journal of Interventional Cardiac Electrophysiology*, vol. 21, pp. 19-26, 2008.
- [15] U. Yasuhiro, "Endoscope," Japanese Patent Publication JP4082529A, March 16, 1992.
- [16] M. S. Banik, D. R. Boulais, L. A. Couvillon, A. C. C. Chin, and I. W. Hunter, "Endoscopic imaging system," U. S. Patent US2004199052A1, October 7, 2004.
- [17] J. Stingl, V. Băca, P. Čech, J. Kovanda, H. Kovandová, V. Mandys, J. Rejmontová and B. Sosna, "Morphology and some biomechanical properties of human liver and spleen," *Surgical and Radiologic Anatomy*, vol. 24, pp. 285-289, 2002.